Software-Defined, WiFi and BLE Compliant Back-Channel for Ultra-Low Power Wireless Communication

Huajun Zhang, David D. Wentzloff, and Hun Seok Kim
EECS, University of Michigan, Ann Arbor, MI, USA, {zhhuajun, wentzlof, hunseok}@umich.edu

***Abstract*—In this paper, we present an innovative back-channel wireless communication concept. The proposed back-channel communication enables ultra-low power (ULP) devices that are neither WiFi (IEEE 802.11a/g/n) nor Bluetooth Low Energy (BLE) compliant to receive messages from both WiFi and BLE transmitters. This allows communication between heterogeneous devices beyond the boundary of WiFi and BLE standards without hardware modification on already-deployed infrastructure. Back-channel messages are created in frequency shift keying (FSK) modulation format by feeding carefully crafted bit sequences in the payload of the WiFi or BLE packets. Systematic algorithms are introduced to embed any desired back-channel messages in FSK format on WiFi and/or BLE compliant packets. Using a commercial off-the-shelf (COTS) narrowband FSK receiver, we demonstrate successful reception of back-channel messages from WiFi and BLE transmitters. Although this COTS narrowband FSK receiver is not specifically designed for the back-channel communication, less than 1% packet error rate (PER) is achieved, validating the concept of software defined back-channel communication among heterogeneous wireless devices.**

I. Introduction

In many ultra-low power (ULP) wireless sensor network applications, wireless communication is the dominant factor in overall power consumption [1]–[4]. The power consumption breakdown of a millimeter scale, energy harvesting sensor node [4] indicates the wireless communication takes more than 65% of overall operating power budget even with aggressive duty cycling. Energy efficient wireless connectivity is one of the most critical issues to prolong the lifespan of wireless sensor network nodes and eventually realize (semi-) perpetual operation only powered by harvested ambient energy.

This paper presents innovative back-channel communication techniques for ULP wireless connectivity. The concept of embedded back-channel communication enables a variety of new applications inter-connecting heterogeneous devices. For example, the proposed scheme allows ULP devices in deep-sleep states that are *not WiFi/BLE compliant* to wake up by back-channel communication embedded in standard WiFi and/or BLE compliant packets. The proposed back-channel signaling has unique properties that are easily detectable by ULP receivers consuming only 100s of μW or even less power.

To demonstrate the back-channel concept, we consider the WiFi (IEEE 802.11 a/g/n) [5] and BLE [6] as the primary target standard, although the proposed technique can be generalized for other standards with similar modulation and coding schemes (e.g. the OFDM based 4G LTE) as well. In the proposed back-channel communication, neither specialized hardware nor a dedicated wireless channel is necessary to send back-channel signals embedded in standard compliant packets. Instead, carefully crafted bit sequences in the payload would generate embedded back-channel signals. That is, back-channel signal transmission is entirely software-defined by simply using a proper data bit sequence for the payload in standard compliant packets. The primary motivation of back-channel communication is to reduce the amount of energy used for wireless communication, while maintaining the ability to communicate with existing wireless infrastructure such as WiFi and BLE networks. This is achieved by using an existing COTS receiver [8] or by designing a dedicated ULP back-channel receiver, which does not have to be compliant with the standard.

In this paper, we will prove the concept of the embedded back-channel signal generation without modifying the existing packet structure of orthogonal frequency division multiplexing (OFDM) based WiFi and Gaussian filtered FSK (GFSK) based BLE. More specifically, we will show binary FSK modulated back-channel communication embedded in OFDM WiFi and GFSK BLE packets. The embedded back-channel signaling is enabled by a set of carefully crafted bit sequences that comply with standard WiFi / BLE packet structure. The proposed concept is depicted in Fig. 1. Note that a standard complaint data receiver can demodulate the entire bit sequence including the back-channel message. Meanwhile, at the back-channel receiver, only the embedded back-channel message is decodable, not the entire bit sequence.

Demodulating a WiFi OFDM signal is a power demanding task (typically $> 120mW$ [9], [11], [12]) due to stringent RF / analog frontend specifications and sophisticated digital base-band processing. Commercial BLE receivers also requires 10s of mW active power consumption [13]–[15] to demodulate $1Mbps$ GFSK signal with inter-symbol interference mitigation techniques to achieve the highest possible sensitivity performance. Although WiFi and BLE signals are ubiquitously available in urban environments, the majority of ULP ($< 1mW$) devices cannot utilize WiFi/BLE connectivity because of their extremely limited power and/or complexity budget [1]–[4], [16]. The proposed back-channel communication technology will break this barrier to allow heterogeneous ULP Internet-of-Things devices to interoperate with already existing WiFi/BLE infrastructure with minimal power consumption ($< 1mW$).

978-1-5090-1328-9/16/$31.00 ©2016 IEEE

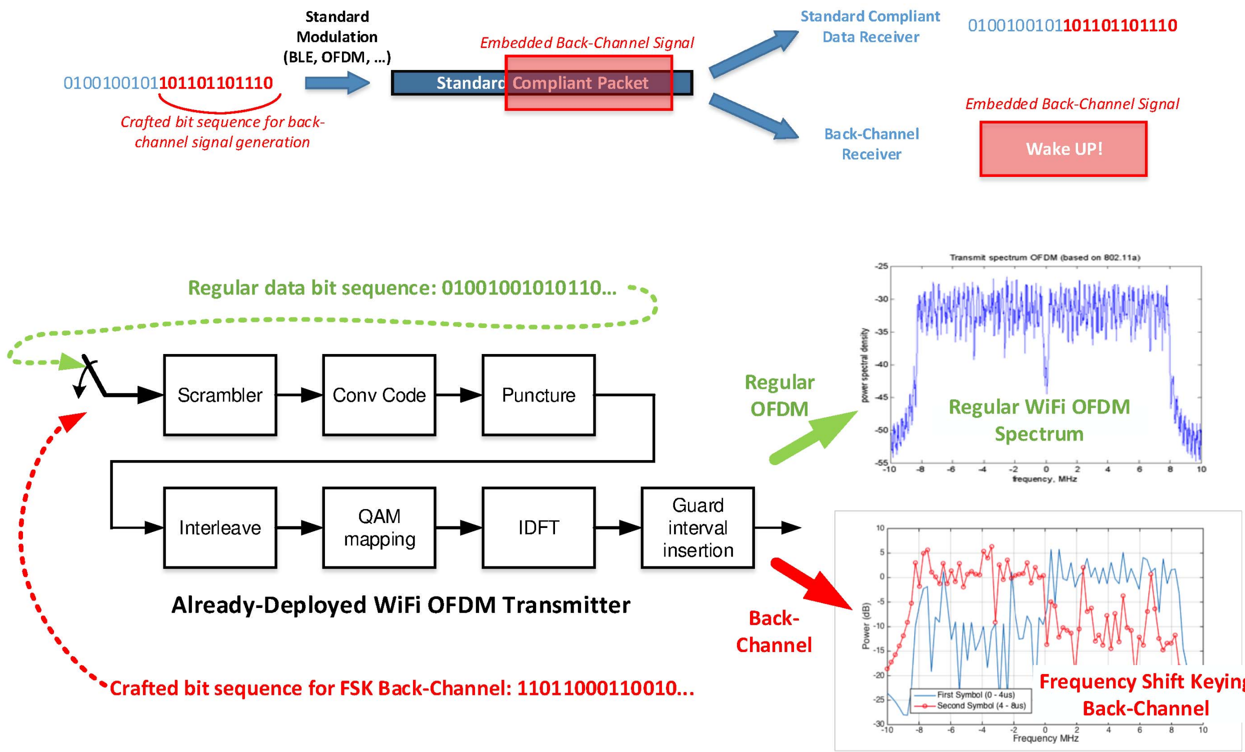

Fig. 1: Concept of WiFi back-channel communication.

Using the back-channel, existing WiFi and BLE devices will be able to control ULP devices which have much more stringent power budget, while not affecting the communication between existing WiFi and BLE devices. The back-channel can be utilized to realize the concept of WiFi/BLE on-demand, where the OFDM/BLE receiver stays in sleep mode until it is waken up through an always-on ULP (10s of μW) wake-up receiver listening to the back-channel. In this way, low latency synchronization between WiFi/BLE links can be maintained while dramatically reducing the average power consumption.

We validated the back-channel concept with a COTS narrowband FSK receiver [8] demodulating FSK modulated back-channel messages generated by standard compliant WiFi and BLE transmitters, all operating in the 2.4 GHz ISM band. Evaluation results show that reliable communication between WiFi/BLE transmitters and a low power FSK receiver is indeed feasible using the proposed concept of back-channel.

II. FSK Back-Channel Modulation in Standard-Compliant WiFi and BLE Packets

In this section we present systematic methods of producing FSK modulated back-channel messages in standard-compliant WiFi and BLE packets.

A. Frequency Shift Keying Back-Channel in WiFi

We first introduce an algorithm to produce FSK modulated back-channel signal in WiFi OFDM packets. For FSK modulated back-channel, we propose intentional non-uniform QAM (quadrature amplitude modulation) symbol power allocation across OFDM subcarriers as shown in Fig. 1 and 2. If arbitrary symbol power allocation for each subcarrier was allowed in the WiFi standard, the back-channel modulation would be straightforward. However, as depicted in Fig. 1, the IEEE 802.11 a/g/n WiFi standard datapath does not allow an arbitrary sequence of QAM symbols. The input data bit stream is scrambled, and encoded with a convolutional code. The coded bit sequence is then punctured, interleaved, and finally mapped to QAM symbols in the WiFi standard datapath. Some subcarriers are assigned as pilot and null subcarriers with predefined modulation symbols. Therefore, only a subset of all possible QAM symbol sequences is WiFi standard compliant. The convolutional encoder output has to be a valid codeword, which is a subset of all possible bit sequences.

Therefore, one can consider the back-channel modulation process in WiFi OFDM as a search problem to identify an input bit sequence that results in a particular QAM symbol sequence whose power allocation is closest to the desired non-uniform FSK back-channel power profile as shown in Fig. 2.

For an M-ary FSK back-channel modulation, we define M non-overlapping subsets of subcarrier indices $\mathcal{S}_{SC}^{(0)}$, $\mathcal{S}_{SC}^{(1)}$,..., $\mathcal{S}_{SC}^{(M-1)}$ satisfying that cardinality of $\mathcal{S}_{SC}^{(m)}$ is M/K for all m, $\mathcal{S}_{SC}^{(m)} \cap \mathcal{S}_{SC}^{(n)} = \emptyset$ for $m \neq n$, and $\mathcal{S}_{SC}^{(0)} \cup \mathcal{S}_{SC}^{(1)} \cup \ \ldots\ \cup \mathcal{S}_{SC}^{(M-1)} = \{1,\ 2,\ ,\ldots K\}$. K is the total number of OFDM subcarriers. A back-channel M-ary FSK symbol m' is created by allocating higher power symbols to

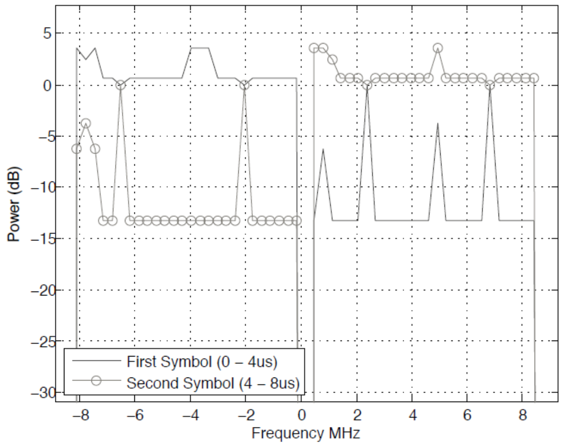

Fig. 2: Realization of binary FSK back-channel modulation.

subcarriers in the subset $S_{SC}^{(m')}$ while lower power is assigned to all other subcarriers. For a binary FSK example, one can use $\mathcal{S}_{SC}^{(0)} = \{1,\ 2,\ \ldots,\ \frac{K}{2}\}$ and $\mathcal{S}_{SC}^{(1)} = \{\frac{K}{2}{+}1,\ \frac{K}{2}{+}2,\ \ldots, K\}$ as depicted in Fig. 2.

Fig. 2 shows a realization of an FSK back-channel OFDM symbol pair in the frequency domain, where two back-channel data bits are modulated by allocating higher power to $\mathcal{S}_{SC}^{(0)}$ for the first OFDM symbol, and higher power to $\mathcal{S}_{SC}^{(1)}$ for the second OFDM symbol. The WiFi OFDM symbol duration is $4\mu s$, thus the binary FSK back-channel modulation in Fig. 2 corresponds $250kbps$ data rate (note that WiFi IEEE802.11a/g/n uncoded data rate is at least $12Mbps$ [5]). The 64-QAM subcarrier symbol constellation was used to realize the example shown in Fig. 2. Non-uniform power allocation within the set $\mathcal{S}_{SC}^{(0)}$ or $\mathcal{S}_{SC}^{(1)}$ is because of the restrictions on a WiFi compliant datapath that includes mandatory convolutional coding and null/pilot subcarriers.

Although ideal (i.e., uniform power allocation) M-ary FSK modulation is infeasible due to WiFi datapath restrictions, the proposed systematic algorithm can circumvent this issue to generate approximated FSK back-channel modulation that is compliant with WiFi standards.

We denote $\mathcal{Q}_k$ as the set of all possible QAM symbols that can be assigned to the subcarrier k. High order QAM constellations such as 64-QAM are recommended to maximize the power difference between the high and low power subcarriers. The $\mathcal{Q}_k$ contains all valid QAM symbols initially. The number of entries in $\mathcal{Q}_k$ decreases as a result of sequentially specifying QAM mapping input bits following the procedure in Algorithm 1. Each QAM mapping input bit assignment for the subcarrier k reduces the size of $\mathcal{Q}_k$ by the factor of $\frac{1}{2}$. The size of $\mathcal{Q}_k$ becomes 1 once all QAM mapping input bits for the subcarrier k are specified.

The back-channel modulation is the process of determining N_{SI} scrambler input bits, $b_0, \ldots, b_{N_{SI}-1}$, for each OFDM symbol. A single back-channel message symbol is created by an OFDM symbol. That is, N_{SI} scrambler input bits need to be specified to generate a back-channel symbol. In

---

Algorithm 1 WiFi payload bit assignment for FSK back-channel modulation. A binary-FSK example assigning higher power to $\mathcal{S}_{SC}^{(high)}$ and lower power to $\mathcal{S}_{SC}^{(low)}$.

1. A WiFi packet must start with mandatory header bits and service bits. The back-channel modulation starts from the third OFDM data symbol.

2. For a back-channel modulated OFDM symbol, the scrambler input bits b_j are determined sequentially from $j = 0$ to $j = N_{SI} - 1$. The index j is initialized to 0. $\mathcal{Q}_k$ for all k is initialized to the set of all possible QAM symbols.

for $(j = 0;\ j < N_{SI};\ j = j + 1)$ **do**

  3. Construct $\mathcal{Q}_k^{b_j=0\ |\mathbf{b_{j-1}}}$ and $\mathcal{Q}_k^{b_j=1\ |\mathbf{b_{j-1}}}$; the set of all possible QAM symbols that can be assigned to the subcarrier k when $b_j = 0$ and $b_j = 1$ respectively, given $\mathbf{b_{j-1}} = [b_0,\ \ldots, b_{j-1}]$ from the result of previous steps.

  4. Evaluate C_0 and C_1 where $C_b = \sum_{\forall k \in \mathcal{S}_{SC}^{(high)}} (P_{MAX} - max\{|\mathcal{Q}_k^{b_j=b\ |\mathbf{b_{j-1}}}|^2\}) + \sum_{\forall k \in \mathcal{S}_{SC}^{(low)}} (min\{|\mathcal{Q}_k^{b_j=b\ |\mathbf{b_{j-1}}}|^2\} - P_{MIN})$, P_{MAX} (or P_{MIN}) is the maximum (or minimum) QAM symbol power among all valid QAM symbols, $|\mathcal{Q}|^2$ is element-wise QAM symbol power on a set $\mathcal{Q}$ and $max\{\mathcal{Q}\}$ (or $min\{\mathcal{Q}\}$) is the operation to select the maximum (or minimum) in a set $\mathcal{Q}$.

  if $C_0 < C_1$ **then**

    5. $b_j \leftarrow 0$

  else

    6. $b_j \leftarrow 1$

  end if

  7. Update the state of the scrambler and convolutional encoder states according to b_j.

end for

8. Repeat from step **2** if there are more back-channel symbols to be modulated. If not, quit.

Algorithm 1, each scrambler input bits are evaluated with a cost function that returns higher value when the scrambler input bit results in further deviation from the desired QAM symbol power allocation. Algorithm 1 assumes the binary FSK modulation assigning higher power to $\mathcal{S}_{SC}^{(high)}$ and lower power to $\mathcal{S}_{SC}^{(low)}$ while $\mathcal{S}_{SC}^{(high)} \cup \mathcal{S}_{SC}^{(low)} = \{1, 2, \ldots, K\}$ and $\mathcal{S}_{SC}^{(high)} \cap \mathcal{S}_{SC}^{(low)} = \emptyset$. Fig. 2 shows binary FSK back-channel modulated OFDM symbols in the frequency domain generated using the proposed Algorithm 1. The presence of pilot and null subcarriers is clearly noticeable in Fig. 2.

B. Frequency Shift Keying Back-Channel in BLE

In this section, we describe a method to generate the binary FSK modulated back-channel embedded in BLE standard compliant packets. The BLE modulation is GFSK at the fixed rate of $1Mbps$. With a goal of achieving significantly lower power consumption and complexity at the receiver, we generate a binary FSK modulated back-channel whose data rate is much lower than the BLE $1Mbps$. Lowering the back-channel symbol rate would reduce power consumption at the

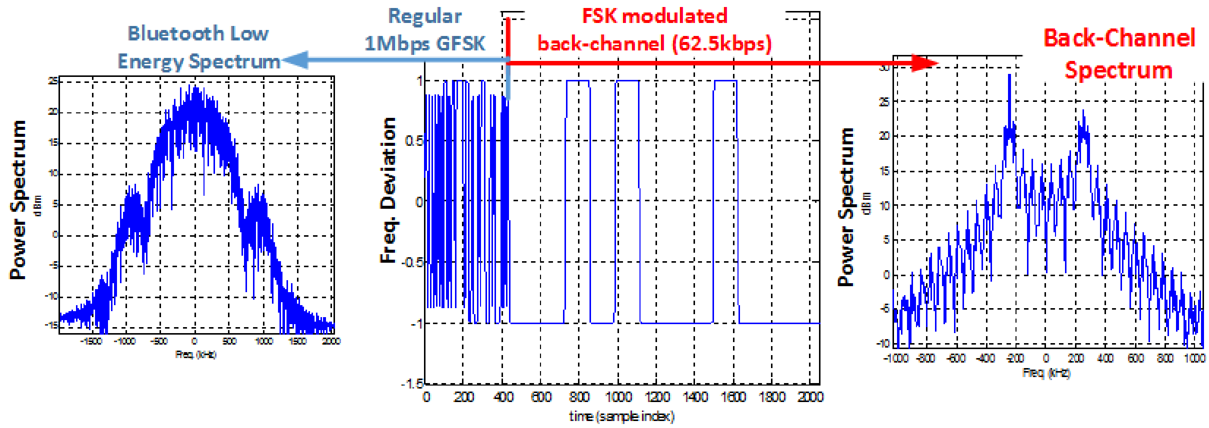

Fig. 3: Back-Channel symbols embedded in a BLE packet and their spectrum.

receiver for the same sensitivity level because the noise power integrated over the signal bandwidth is reduced and digital baseband processing could run at a slower clock frequency.

The BLE standard [6] does not specify a slower data rate than $1Mbps$. However, back-channel symbols with much longer duration than $1\mu s$ can be created by repeating multiple BLE symbols as shown in Fig. 3. The same consecutive N-bits in the BLE packet generate a logical back-channel symbol with the length of $N\mu s$. Since the BT product constant for the BLE Gaussian filter is defined with respect to the original BLE symbol length ($1\mu s$), the Gaussian filter support length becomes relatively insignificant as the logical back-channel symbol duration increases. In other words, the original BLE GFSK modulation is well approximated to a conventional binary FSK when longer back-channel symbols are used. As shown in Fig. 3, frequency transition at the back-channel symbol boundary occurs in a negligible time relative to a back-channel symbol duration ($N\mu s$, $N \gg 1$). The frequency spectrum of a back-channel signal embedded in a BLE packet is shown in Fig. 3. It is clearly noticeable that back-channel symbols are well approximated to binary FSK with $500kHz$ tone spacing (i.e., $250kHz$ frequency deviation). Unlike the original $1Mbps$ GFSK, the inter-symbol interference is no longer relevant in back-channel symbol demodulation. Therefore, it is possible to realize a back-channel receiver to detect embedded back-channel symbols consuming only a fraction of the power required by a regular BLE data receiver. The comprehensive ULP wireless receiver IC survey [7] indicates that 100s of μW power budget is sufficient to design a ULP binary FSK back-channel receiver at 10s - 100s of $kbps$ data rate. For instance, a narrowband FSK receiver [17] reports $350\mu W$ power consumption for $-86dBm$ sensitivity.

The BLE datapath involves a whitener, whose role is to scramble the data bit stream with a pseudo random sequence. The BLE whitener architecture is given in Fig. 4. Its purpose is to avoid consecutive 1s or 0s over multiple symbol durations – exactly what we need to generate the proposed back-channel symbol. In order to create back-channel symbols

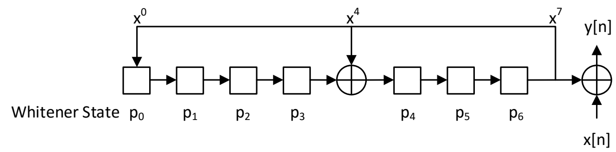

Fig. 4: BLE scrambler [6].

Algorithm 2 BLE data bit $x[n]$ assignment for given back-channel message $m_0, m_1, \ldots, m_{M-1}$. M is the total number of back-channel message symbols. N is the number of BLE symbols to create each back-channel symbol.

1. The whitener state p_i, $i = 0, \ldots, 6$ are initialized according to the BLE channel index, preamble and access address.
2. For back-channel modulation, the whitener input bits $x[n]$ are determined sequentially from $n = 0$ to $MN - 1$. The symbol index n is initialized to 0.
for $(n = 0;\ n < MN;\ n = n + 1)$ **do**
  3. $x[n] \leftarrow m_{\lfloor n/N \rfloor} \oplus p_6$
  4. Update the whitener state: $tmp \leftarrow p_6$, $p_6 \leftarrow p_5$, $p_5 \leftarrow p_4$, $p_4 \leftarrow p_3 \oplus tmp$, $p_3 \leftarrow p_2$, $p_2 \leftarrow p_1$, $p_1 \leftarrow p_0$, $p_0 \leftarrow tmp$
end for

from the whitened bit stream, a purposefully sequenced bit stream needs to be fed as the whitener input. The whitening operation is given by $y[n] = x[n] \oplus p[n]$, where $x[n]$, $y[n]$ and $p[n]$ represents the whitener input (i.e. payload data), output (i.e., GFSK modulator input) and pseudo random sequence respectively with bit index n. The symbol $\oplus$ denotes XOR.

In fact, the pseudo random sequence $p[n]$ is deterministic given the initial state of the whitener. Using the BLE channel index as the initial state, the whitening operation is easily invertible by taking $x[n] = y[n] \oplus p[n]$, where $y[n]$ is the desired whitened bit sequence to create the back-channel.

The procedure to generate binary FSK modulated back-channel messages embedded in a BLE packet is detailed in

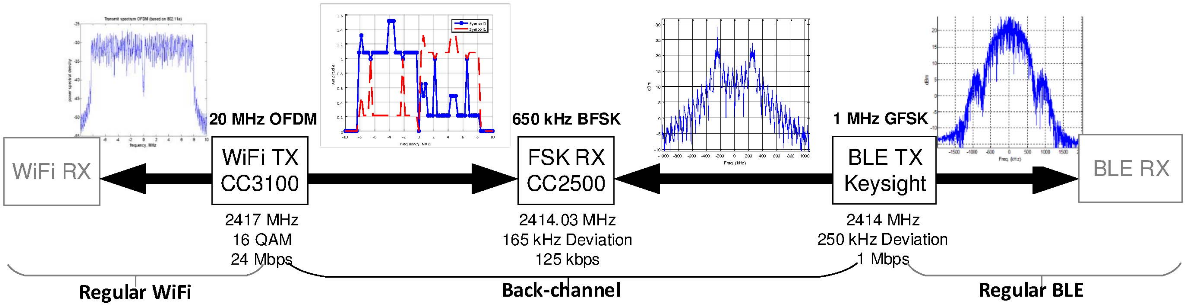

Fig. 5: Back-channel testing setup.

Algorithm 2. Note that the back-channel symbols are located in the PDU part of the BLE packet [6], which appears after the preamble and access address. The maximum length of the PDU is 39 bytes. By using N-consecutive bits for a back-channel symbol, the number of back-channel symbols embedded in a single BLE packet is $312/N$ while its symbol rate is reduced to $\frac{1}{N}$ $Mbps$ from the original BLE $1Mbps$. Fig. 3 shows an example case of $N = 16$.

III. Prototype System Evaluation

A. Evaluation Setup

The proposed back-channel communication receiver is prototyped using a commercial 2.4GHz proprietary FSK receiver, TI CC2500 [8]. To generate back-channel messages embedded in WiFi and BLE packets, we use a commercial WiFi transmitter, TI CC3100 [9] and a standard-compliant BLE transmitter that is software implemented using a Keysight arbitrary signal generator (AWG) [10]. The BLE compliant functionality has been validated through data reception on a BLE protocol analyzer and a smartphone.

Fig. 5 shows the prototype system hardware setup to validate the back-channel communication. The payload bit sequences for WiFi and BLE back-channel modulation are identified using Algorithm 1 and 2, respectively. For back-channel communication, the external host (TI MSP430 Microcontroller) feeds the crafted payload bits to the TI CC3100 WiFi transceiver and/or Keysight AWG based BLE transmitter. Note that no hardware modification or API function changes are required for the WiFi / BLE transmitter for back-channel transmission.

We configured the TI CC2500 2.4GHz proprietary FSK receiver chip to receive FSK modulated back-channel messages from both WiFi *and* BLE transmitters. To match the data-rate between the transmitter and receiver, two WiFi OFDM symbols are grouped together to create a single back-channel bit, realizing a back-channel data rate of $125kbps$. BLE back-channel parameter N (number of BLE symbols per back-channel bit) is set to 8 to achieve the same back-channel data rate. It is worth noting that we include preamble and sync word bytes in the back-channel modulated message to help automatic gain control and synchronization performed at the CC2500 receiver. The sync word also identifies a specific receiver for the message. In order to create a sizable back-channel packet including the preamble and sync word, 16-QAM modulation is chosen instead of 64-QAM for WiFi transmission. This corresponds to the $24Mbps$ mode in IEEE 802.11g standard. Using 64-QAM WiFi transmission would decrease the maximum length of the back-channel message since each OFDM symbol requires more WiFi payload bits. The back-channel message packet in the proposed prototype system contains 3-byte preamble, 2-byte sync word, and 2-byte message. 2-byte back-channel message is sufficient for demonstrating short commands such as wake-up.

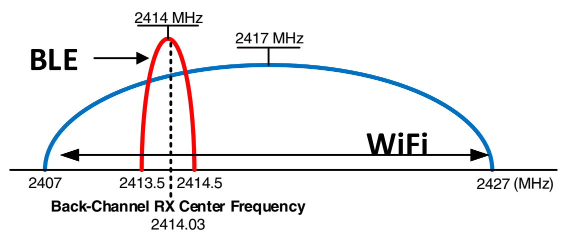

Fig. 6: Frequency plan of WiFi and BLE back-channels.

Fig. 6 shows the frequency configuration of WiFi and BLE back-channels. This particular frequency plan allows the CC2500 FSK receiver to receive back-channel messages from both WiFi *and* BLE without changing its demodulation parameter configuration. The WiFi center frequency is defined by $2417+10n\ MHz,\ n = 0, 1, \ldots, 5$, while BLE channel center frequencies are $2402 + 2n\ MHz,\ n = 0, ..., 39$. Note that the WiFi back-channel center frequency does not have to be aligned with the WiFi center frequency. Using Algorithm 1, the FSK back-channel center frequency can be arbitrarily chosen. In our experiments, the center frequency of the CC2500 FSK receiver (i.e., the back-channel center frequency) is set in the middle of two adjacent WiFi subcarriers with index -9 and -10 as shown in Fig. 6. The frequency deviation of the CC2500 FSK receiver chip is set to approximately half of the WiFi subcarrier spacing, $312.5/2 = 165.25kHz$. Using this frequency setup, it is possible to put a BLE channel

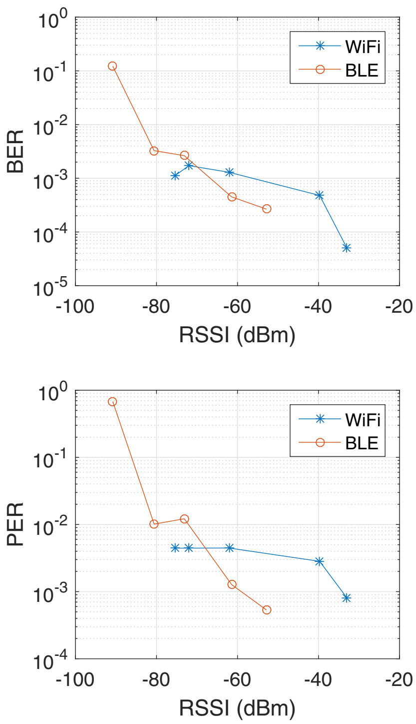

Fig. 7: BER and PER vs. RSSI for WiFi and BLE backchannels.

center frequency only $30kHz$ away from the carrier frequency of the CC2500 FSK chip. This $30kHz$ frequency offset is within the frequency drift tolerance of the CC2500 FSK receiver. Although BLE and WiFi back-channel have different frequency deviations ($250kHz$ and $165.25kHz$, respectively), we have validated that the CC2500 FSK receiver is able to demodulate back-channel packets from both WiFi and BLE devices without demodulation parameter modification.

B. Measurement Results

The back-channel communication was successfully validated in wireless testing conducted in a university lab environment. To quantify the performance, bit error rate (BER) and packet error rate(PER) are measured in a wired setting where we can precisely control the received signal power (RSSI) using attenuators. Both WiFi and BLE transmitters are configured to repeatedly transmit the same packet. The received messages are recorded, and then compared with the transmitted message to measure BER and PER. Fig. 7 shows the actual BER/PER measurement results. Although CC2500 FSK chip is not specifically designed for back-channel communication, it can achieve 10^{-2} or lower PER for both WiFi and BLE back-channel when the received signal power level is higher than -75dBm. These experiments validate the feasibility of the proposed back-channel communication concept. The CC2500 receiver consumes less than 20 mW [8], which is 6x lower than WiFi receivers. We expect significantly better PER performance and/or power efficiency by designing a custom receiver optimized for the proposed back-channel modulation and its packet structure.

IV. Conclusion

In this paper, the concept of back-channel communication embedded in WiFi and BLE compliant packets is proposed. Systematic algorithms are presented to generate FSK back-channel modulation within WiFi and BLE packets. The proposed back-channel communication concept is validated through a prototype system built on commercial standard-compliant WiFi and BLE transmitters and a proprietary FSK receiver. Measurement results show that reliable back-channel communication is feasible between heterogeneous device beyond the WiFi and BLE standard boundary.

References

[1] I. Demirkol, C. Ersoy, and E. Onur, "Wake-up receivers for wireless sensor networks: benefits and challenges," *Wireless Communications, IEEE*, vol. 16, no. 4, pp. 88–96, Aug 2009.

[2] L. Gu and J. Stankovic, "Radio-triggered wake-up capability for sensor networks," in *Real-Time and Embedded Technology and Applications Symposium, 2004. Proceedings. RTAS 2004.*, pp. 27–36.

[3] J. Ansari, D. Pankin, and P. Mahonen, "Radio-triggered wake-ups with addressing capabilities for extremely low power sensor network applications," in *Personal, Indoor and Mobile Radio Communications, 2008. PIMRC 2008. IEEE 19th International Symposium on*, Sept 2008.

[4] G. Chen, H. Ghaed, R. u. Haque, M. Wieckowski, Y. Kim, G. Kim, D. Fick, D. Kim, M. Seok, K. Wise, D. Blaauw, and D. Sylvester, "A cubic-millimeter energy-autonomous wireless intraocular pressure monitor," in *Solid-State Circuits Conference Digest of Technical Papers (ISSCC), 2011 IEEE International*, Feb 2011, pp. 310–312.

[5] *IEEE 802.11n specification*. [Online]. Available: https://standards.ieee.org/findstds/standard/802.11n-2009.html

[6] *Bluetooth Core Specification 4.0*. [Online]. Available: https://www.bluetooth.org/en-us/specification/adopted-specifications

[7] D. D. Wentzloff, "Low power radio survey," [Online]. www.eecs.umich.edu/wics/wp-content/low_power_radio_survey.html

[8] Texas Instruments, *CC2500 Datasheet*. [Online]. Available: http://www.ti.com/lit/ds/symlink/cc2500.pdf

[9] Texas Instruments, *CC3100 Datasheet*. [Online]. Available: http://www.ti.com/product/CC3100/datasheet

[10] Keysight, *N5182A Vector Signal Generator*. [Online]. Available: http://literature.cdn.keysight.com/litweb/pdf/5989-5261EN.pdf?id=840899

[11] T.-M. Chen, et. al., "A low-power fullband 802.11a/b/g WLAN transceiver with on-chip PA," *Solid-State Circuits, IEEE Journal of*, vol. 42, no. 5, pp. 983–991, May 2007.

[12] M. Zargari, et. al., "A single-chip dual-band tri-mode CMOS transceiver for IEEE 802.11a/b/g WLAN," in *IEEE International Solid-State Circuits Conference, 2004*, Feb 2004, pp. 96–515 Vol.1.

[13] Texas Instruments, *CC2640 Datasheet*. [Online]. Available: http://www.ti.com/lit/ds/symlink/cc2640.pdf

[14] T. Sano, et. al., "13.4 a 6.3mW BLE transceiver embedded RX image-rejection filter and TX harmonic-suppression filter reusing on-chip matching network," in *Solid- State Circuits Conference - (ISSCC), 2015 IEEE International*, Feb 2015, pp. 1–3.

[15] Y. H. Liu, et. al., "13.2 a 3.7mw-RX 4.4mw-TX fully integrated Bluetooth Low-Energy/IEEE802.15.4/proprietary SoC with an ADPLL-based fast frequency offset compensation in 40nm CMOS," in *Solid-State Circuits Conference - (ISSCC), 2015 IEEE International*, Feb 2015.

[16] Y. Lee, G. Kim, S. Bang, Y. Kim, I. Lee, P. Dutta, D. Sylvester, and D. Blaauw, "A modular 1mm3 die-stacked sensing platform with optical communication and multi-modal energy harvesting," in *Solid-State Circuits Conference Digest of Technical Papers (ISSCC), 2012 IEEE International*, Feb 2012, pp. 402–404.

[17] J. Ayers, N. Panitantum, K. Mayaram, T.S. Fiez, "A 2.4GHz wireless transceiver with 0.95nJ/b link energy for multi-hop battery-freewireless sensor networks," in *IEEE Symposium on VLSI Circuits (VLSIC)* 2010, pp.29 - 30, 16-18 June 2010